Atmospheric Environment 312 (2023) 119992

Contents lists available at ScienceDirect

Atmospheric Environment

journal homepage: www.elsevier.com/locate/atmosenv

Tracing the origin of odour nuisance from citizens' notifications with the SMART modelling system

Silvia Trini Castelli [a,*], Francesco Uboldi [b,1], Gianni Luigi Tinarelli [c], Oxana Drofa [d], Piero Malguzzi [d], Paolo Bonasoni [d]

[a] Institute of Atmospheric Sciences and Climate, National Research Council, Torino, Italy
[b] International Center for Environmental Monitoring, CIMA Foundation, Savona, Italy
[c] ARIANET Srl, Milano, Italy
[d] Institute of Atmospheric Sciences and Climate, National Research Council, Bologna, Italy

GRAPHICAL ABSTRACT

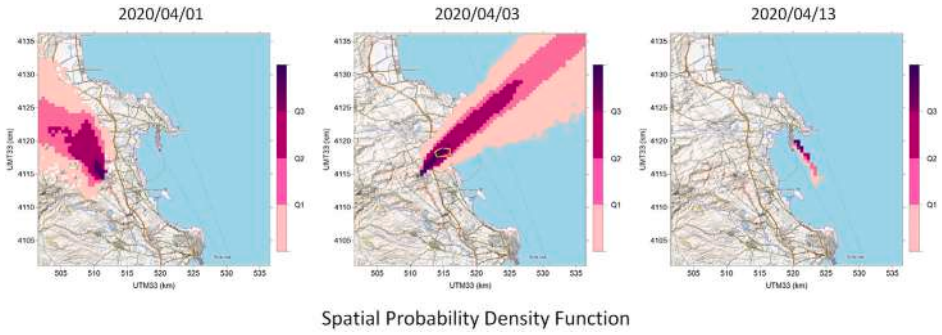

HIGHLIGHTS

- Citizen cooperation in support to odour nuisance tracing.
- Lagrangian backward numerical modelling to identify source areas.
- A new approach to use citizens' notifications as input to numerical model simulations.
- A new methodology to elaborate probability distribution maps of source locations.

ARTICLE INFO

Keywords:
Odour nuisance
Backward dispersion
Unknown source tracking
Numerical simulation
Local-regional scale
NOSE Web-App
SMART modelling system

ABSTRACT

Odour nuisance has a not negligible impact on the quality of life of the population affected by it, yet tracing the source of malodorous releases is challenging. Numerical models may be profitably used, to support both the identification of the potential source areas and the execution of timely field measurements. In this frame, a new methodology has been developed with the aim of tracing backward the origin of odour nuisance, starting from citizens' notifications. A numerical procedure processing the alerts received through the Web-App NOSE, has been developed to produce the proper input to the dispersion module of the SMART meteo-dispersive modelling system. Then, a post-processing numerical code elaborates the simulation output based on a combination of puffs of Lagrangian stochastic particles, released backward in time from the locations and at the time of the citizens' notifications. This novel approach is presented, it is applied to three real case studies occurred in the area of Siracusa province (Sicily, Italy), then related results are discussed. The new methodology proved to be reliable and effective in identifying the most probable zones that can originate the nuisance.

* Corresponding author.
E-mail address: s.trinicastelli@isac.cnr.it (S. Trini Castelli).
[1] Previous affiliation: ARIANET Srl Milano, Italy.

https://doi.org/10.1016/j.atmosenv.2023.119992
Received 8 January 2023; Received in revised form 24 July 2023; Accepted 31 July 2023
Available online 7 August 2023

1. Introduction

The release and transport of disturbing odorous substances in the atmosphere, generated from various activities, like industry, agriculture, waste management and treatment, imply a nuisance for the population and may even entail health effects. In air pollution context, dealing with odours represents a challenge due to their transient and volatile characteristics. Odours are produced by a mixture of substances and often nuisance events are connected to brief peaks of concentration, making them barely detectable. It becomes thus difficult to devise dedicated monitoring systems and networks.

In such frame, numerical models in general, and Lagrangian particle dispersion models in particular, can be profitably used for tracing the provenience and emission sources of odours. In the Lagrangian approach, the simplest method to seek for potential release areas is based on back-trajectories, which can be purely deterministic or stochastic. In the first case, the single trajectory of a tracer parcel is reconstructed from the receptor point backward in time following the mean flow, that is moving it accounting only for the mean wind velocity and neglecting turbulent diffusion. While deterministic trajectories can be considered an acceptable approximation over the long range, it may become too rough at the local and regional scale. To account for the atmospheric turbulence, the most advanced approach in Lagrangian modelling is using stochastic 'virtual' particles, whose dispersion is determined both by the mean flow, that is the local wind, and its fluctuations, given by random velocities obtained as solution of Lagrangian stochastic differential equations.

Backward trajectories, using both Lagrangian and Eulerian models, are applied to identify the zones of origin of different types of tracers, from pollutant gases to radioactive substances, dust, greenhouse gases and even odours (Flesch et al., 1995; Chiapello et al., 1997; Pudykiewicz, 1998; Elbern et al., 2007; Gurney et al., 2002; Hourdin and Talagrand, 2006; Kopacz et al., 2009; Schauberger et al., 2011; Thompson et al., 2014; Bergamaschi et al., 2015; Ferrarese and Trini Castelli, 2019).

Simply tracing backward trajectories from measured concentrations provide a qualitative information about the reconstruction of possible emitting sources. A further development of the approach is represented by the Source Term Estimation (STE) algorithms (Platt and DeRiggi, 2012; Hutchinson et al., 2017). In STE algorithms, concentration measurements of chemical species or odour units, are used as input to dispersion models applied in their backward mode. In fact, every receptor point is considered as a releasing source and the dispersion of the tracer is followed backward in time, upwind. Any dispersion model can be used in such approach, from simple Gaussian to more advanced Lagrangian and Eulerian models, where the advection is simulated backward in time and the module solving the turbulent diffusion is properly modified. Because of the intrinsic variability and uncertainty of the atmospheric dispersion processes and of their numerical simulation, the patterns obtained by modelling in backward mode the dispersion of tracers measured at different receptor points and different times, may correspond to areas of origin that do not overlap or are even contrasting. In STE approach, a post-processing of the backward simulations is applied, to integrate all available information and identify a possible release area that is congruent with all outcomes. Using measured concentrations at the receptors, this method allows providing an estimation of the location, emission rate, time of release and related uncertainty of the unknown source. The post-processing may be based on a simple statistical elaboration counting maximum overlap of concentration fields produced by the backward simulations or applying variational methods to minimise the values of an objective function (Tinarelli et al., 2018), or on a Bayesian approach (Rajaona et al., 2015).

In recent years, the web-application NOSE (Network for Odours Sensitivity, see https://nose-cnr.arpa.sicilia.it/) was realised by CNR-ISAC and ARPA Sicilia, with the purpose of investigating and tracking episodes of odour nuisance in the highly industrialised area of Siracusa province in Sicily through a citizen-science approach. Starting from the nuisance notifications received through the Web-App, the SMART modelling system (Bisignano et al., 2020) has been adapted for its implementation in NOSE, to support backtracing the potential location of the odour emission. SMART is composed by the offline interface of the regional meteorological model MOLOCH (Malguzzi et al., 2006) and the Lagrangian particle dispersion model SPRAY (Tinarelli et al., 2000) through the parameterisation code ARAMIS (Bisignano and Trini Castelli, 2018). In application to NOSE, SMART makes use of RetroSPRAY (Tinarelli et al., 2018), the version of SPRAY capable of simulating the dispersion backward in time of a plume or puff released by a source. A puff corresponds to a short-time emission (compared to the flying time of the released substance), while a plume refers to a continuous emission, a sum of several puffs. Hereafter we use the prefix 'retro' to indicate puffs, emissions and sources that refer to a backward-in-time simulation. A novel methodology has been developed to (i) process the NOSE alerts in order to prepare the proper input to the dispersion model RetroSPRAY, and (ii) elaborate its output to provide a clear information on the possible location of the source. The approach builds around three phases. The citizens' qualitative and subjective alerts are grouped and selected on the basis of sensible criteria to generate pseudo-receptors, in fact location and times of "retro-emissions" for the back-trajectories of the Lagrangian particles. Then, simulation with SMART system are performed, producing the meteorological fields for the period of the event and releasing, in RetroSPRAY run, a series of "retro-puffs" from the identified receptors at each time interval in which the number of alerts is larger than a given threshold. In a RetroSPRAY simulation, Lagrangian particles are released at retro-sources locations and their individual retro-trajectories are calculated, backward in time and upwind. Then, at each unit time interval, the fields of the "backward concentration" generated by the retro-puffs (hereafter named as "retro-puff fields") are calculated by counting the Lagrangian particles that, in that time interval, are present within each grid-box of the integration domain. Finally, the retro-puff fields calculated by RetroSPRAY are combined, through a process that produces maps describing the region where the odour source can be potentially located and its related probability density.

In this work, the novel methodologies in SMART modelling system and NOSE Web-App are presented and applied. The application of the new approach is discussed based on the results obtained in three case studies, characterised by a different number of notifications, different meteorological and release conditions and different levels of complexity.

In Sections 2 and 3 the SMART modelling system and the NOSE Web-App are briefly presented, respectively. In Section 3 also the three selected case studies are introduced. Section 4 presents and discusses the new methodology developed to elaborate the input and output for SMART simulations, till the final outcome represented by the maps. In Section 5 the results of the application of the methodology and of the SMART simulations are reported and discussed, while conclusions on the reliability and efficacy of the approach are drawn in Section 6.

2. Brief description of SMART modelling system

The SMART (SPRAY-MOLOCH Atmospheric Regional Tool) modelling system has been created with the initial aim of making available a modelling suite that can forecast the dispersion of possible accidental releases in any part of the Italian territory at any time (Bisignano et al., 2020; Trini Castelli et al., 2020; Bisignano and Trini Castelli, 2021). This approach is feasible thanks to the daily numerical forecasts issued by the chain of meteorological models, GLOBO (Malguzzi et al., 2011) - BOLAM (Buzzi et al., 1994, 2004) - MOLOCH (Malguzzi et al., 2006), operating from the global to the regional scale and developed by the MODAT modelling group at CNR-ISAC. At the regional scale, the MOLOCH model integrates the non-hydrostatic, fully compressible

equations for the atmosphere and produces meteorological forecasts with spatial resolution of 1.25-km grid step for the full Italian territory (http://www.isac.cnr.it/dinamica/projects/forecasts/moloch/). In SMART applications, MOLOCH simulations are typically performed at a grid resolution of 0.5 km.

Starting from the availability of these high-resolution forecasts, a new parameterisation code, ARAMIS (Bisignano and Trini Castelli, 2018, Atmospheric Regional Algorithm for Moloch Interfaced to Spray), was developed to interface the MOLOCH meteorological model with the Lagrangian particle dispersion model SPRAY (Tinarelli et al., 1994, 2000). ARAMIS sets up the domain of interest, reads the variables from MOLOCH outputs, given on a grid in geographical coordinates, elaborates and interpolates them on a regular grid in UTM coordinates, calculates the turbulent variables needed by the Lagrangian particle model, such as the wind velocity standard deviations and the Lagrangian time scales, and prepares the input for SPRAY model.

SPRAY is an advanced Lagrangian particle dispersion model, widely applied and validated in a number of case studies. In it, the mean motion of the virtual particles is defined by the local wind and the dispersion is determined solving the Langevin stochastic differential equations for the wind velocity fluctuations. This enables reproducing the statistical characteristics of the turbulent flow, since portions of the plume emitted by a source may experience different atmospheric conditions, thus reproducing in a realistic way the complexity of the atmospheric processes. SPRAY accounts for the complex topography and the heterogeneous landuse (Carvalho et al., 2002; Nanni et al., 2022), also in presence of obstacles with its microscale version (Tinarelli et al., 2012; Trini Castelli et al., 2018), and specific modules are implemented to treat the particular low-wind speed conditions (Anfossi et al., 2006) and the dynamics of dense-gas releases (Anfossi et al., 2010).

The SMART modelling system, composed by MOLOCH, ARAMIS and SPRAY, has been applied to some test cases – see for instance Bisignano et al. (2020), Bisignano and Trini Castelli (2021) – and demo of simulations were proposed for two accidental fires occurring in Italy in 2020 (see https://www.isac.cnr.it/en/news/smart-simulation-fire-3v-sigma-plant-marghera-venice-may-15th-2020 and https://www.isac.cnr.it/en/news/smart-simulation-fire-harbour-ancona-september-16th-2020).

Beyond the simulation of atmospheric pollutant dispersion in case of accidental releases, SMART suite can be adapted and adopted to trace back the location of a possible unknown source of unidentified releases. In the frame of the present work, a new development pertained to SMART modelling system, where a version of the SPRAY model that includes the option for back-trajectories, RetroSPRAY (Armand et al., 2013; Tinarelli et al., 2018), has been implemented. For typical airborne pollutants, having available observed concentrations, in RetroSPRAY the plausible location of an unknown source can be estimated with two approaches: in the first case, by identifying areas with maximum spatial and temporal consistency among backward trajectories from each sensor; in the second, a variational method is used to minimise the estimate-observation residual at each grid-box reached by backward trajectories, providing information on the source location and time, emitted quantities and related uncertainty.

In dealing with odour emissions, given that they are often composed by a mixture of different substances and are characterised by peak events of nuisance that may last for a short period, generally observed concentrations are not available or not available promptly enough. An input that can potentially be used as receptor for tracing back-trajectories is represented by the citizens' complaints, when they can be registered through a notification and alert system. In implementing RestroSPRAY in SMART system, new and original developments regarded the elaboration of this type of information as input to the model (Uboldi et al., 2022), and the elaboration of the output produced for the application of the system to track the possible origin and source of odour releases (Trini Castelli et al., 2022). The specific description of these developments and their verification in case studies represent the core of the present work.

3. The NOSE project and the case studies

The alert-system NOSE, Network for Odours Sensitivity (https://nose-cnr.arpa.sicilia.it/), has been realised by CNR-ISAC and ARPA Sicilia with the aim of investigating and tracking episodes of odour nuisance, through a citizen-science approach. The NOSE system has been implemented for the region of the Siracusa Province in Sicily (Italy), including a large industrial area located along the coast and the port of Augusta (Fig. 1), an area that includes the largest petrochemical plant in Europe. A Web-App is made available to registered, but untrained, citizens, who can submit their notification at the time and location when and where the nuisance is occurring, with the option to include details on the type of odour, its intensity, the perceived annoyance and to provide additional comments. The data are then collected and processed producing a text file that contains: date, latitude, longitude, name of the region, intensity of the odour (based on a scale from 1 to 5), type and name of the perceived smell (based on list of substances associated to a code), other possible odour type they may identify, description of the type of discomfort symptoms, a list of specific discomfort symptoms the citizens may mark to feel (coded as yes=1, no=0), free comments on the feeling of illness they may perceive. From September 2019 to December 2022 over 3900 citizens of the Province of Siracusa have reported over 12,500 odour nuisance events.

Starting from these data, on NOSE Web-App operational side at present the notifications are grouped on a regular grid over the affected region, as in Fig. 2. Then, to identify the area of possible sources, deterministic back-trajectories, originating from the active grid cells, are traced using MOLOCH meteorological model. The recent development of the modelling suite SMART offers the opportunity to improve the detection of the odour origin based on a full meteo-dispersive system, thus accounting for the stochastic nature of the turbulent atmospheric flow. Specific and new pre- and post-processing modules have been designed in order to use the citizens notifications as input to SMART modelling system, and to elaborate an output that can be informative on the odour origin even on a quantitative viewpoint. The novel methodology is explained and detailed in the following Section 4.

To apply, test and verify the chain of elaboration and simulation in NOSE, three case studies referring to odour nuisance events characterised by different conditions have been considered. They refer to the month of April 2020, during which several episodes occurred, and are briefly detailed in the following.

Case 1, on the 13th of April (tagged 20200413): this event is characterised by an extremely high number of notifications received by the NOSE Web-App, 840 starting around 0500 UTC (= CEST - 2) along all day, 800 from the city of Augusta and 754 of them between 0600 and 1010 UTC . Such clear evidence of the nuisance and the large information available represent an ideal application of the methodology (see the report in https://www.arpa.sicilia.it/oltre-800-segnalazioni-su-nose-ad-augusta-sr-il-13-aprile-lanalisi-dei-dati/).

Case 2, on the 3rd of April (tagged 20200403): in this case the number of notifications is small, 21 from 1820 to 2120 UTC, thus representing a more challenging situation. It provides a good benchmark to verify the reliability of the proposed methodology because the source of the release was identified after field measurements (see the report in https://www.arpa.sicilia.it/picco-di-segnalazioni-di-cattivi-odori-a-melilli-sr-risultati-campionamenti-e-controlli/).

Case 3, on 1st of April (tagged 20200401), is the most challenging: a few notifications were received, 27 from 1240 to 1440 UTC, and rather sparse because coming from detached areas. A sharp change in the wind field characterises the circulation in the area during the event, which may explain the spotted distribution of the notifications (see Fig. 12 in Section 5 and the Animation_WindField_01042020.gif in the Supplementary Material).

The diversity of the three events puts the developed approach to a severe test and allows evaluating its potentiality in detecting the source areas of odour nuisance. The results of the application of the methodology and the outputs of the SMART simulations for the three case studies are reported and discussed in Section 5.

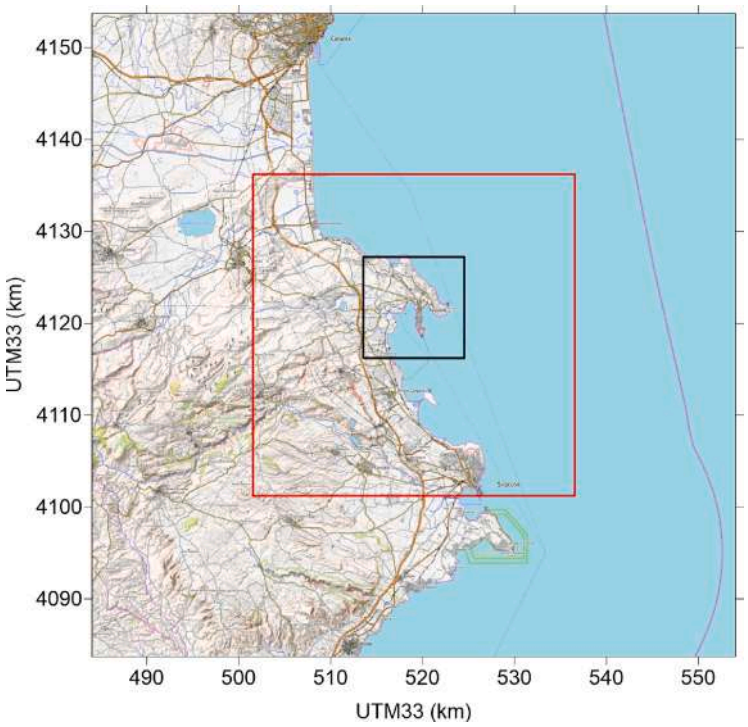

Fig. 1. Map of the SMART simulation domain, covering the area from 14.82° to 15.61° in longitude and 36.90° to 37.53° in latitude. The red and black squares indicate the zoomed-in domains used in Figs. 5, 6, 7, 8, 11, 12, 13 and Figs. 3, 4, 9, 10, respectively.

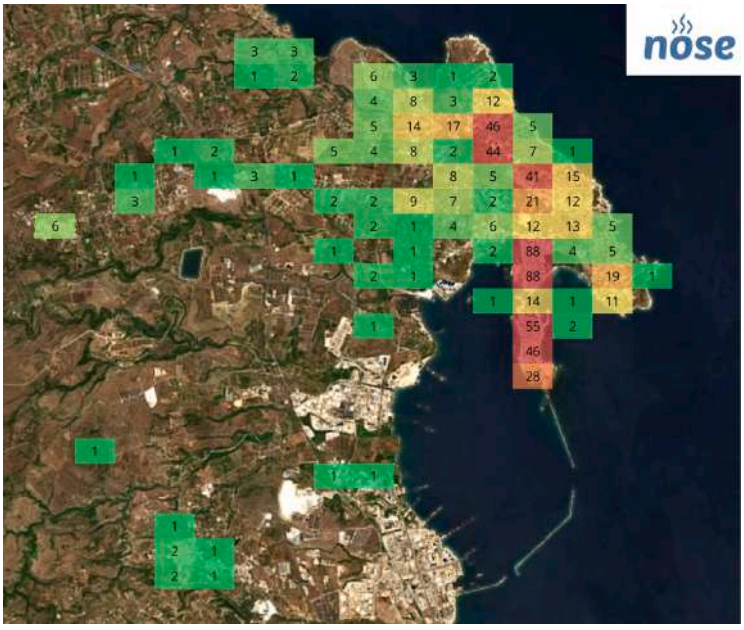

Fig. 2. NOSE Web-App. Example of the grouping into a regular grid of the citizens' notifications: from the active cells the MOLOCH model back-trajectories are originated. The area in the plot roughly corresponds to the domain of the black square in Fig. 1.

4. New developments for tracing back the sources of odour nuisance

The approach designed for tracing back the potential sources of odour nuisance finds its support in the citizen science and its novelty in using the citizens' notifications as direct input for the model simulations.

In SMART system, to simulate the dispersion of tracers the meteorology and the source term are needed. The 3D fields from MOLOCH atmospheric model are processed by ARAMIS turbulence and boundary-layer parameterisation code, in order to elaborate the meteorological input for RetroSPRAY. Here, the new challenge is using the notifications from citizens in place of observed concentrations as input receptors for RetroSPRAY dispersion model. The notifications received through the NOSE Web-App are sparse in space and time, yet they

can be considered as a mobile receptor grid. The idea is to implement a clever grouping or clustering of the alerts for generating proper "receptors" for the back-trajectories. Simulations with RetroSPRAY can then be performed by releasing, from the identified receptors, a series of retro-puffs at each time interval in which a significant number of notifications are collected. In the following subsections, the methodology for the elaboration of both the input and output for SMART modelling system in application to NOSE Project is presented and discussed.

4.1. Elaboration of the input

In order to generate proper receptor-points for the release of backward puffs in RetroSPRAY simulation, a clever elaboration of the information received through the notifications of the citizens is needed. While the time and location of the notifications are retained as actual data, the additional information is clearly characterised by a subjective evaluation of the odour intensity, of the gravity of the following disturbances and effects on health. Therefore, criteria for selecting and properly aggregating the notifications are to be established in order to produce a sensible input to the dispersion model.

In our approach, alerts with intensity 3, 4 or 5 have been used. The peak in the notifications can be considered the signal of the peak of the nuisance event, usually lasting a few or some hours. This enables identifying the period of time determining the event, period that is divided in 30-minutes intervals: all notifications within the same time interval are associated at the same discrete time, which is representing the emission sub-period. Then, the notifications are spatially aggregated to define the "pseudo-receptor" location. In the development of the methodology, this has been done in two alternative ways.

In the first case, a 500-m-spacing regular grid is defined on the domain and the alerts exceeding the established odour intensity threshold (equal to 2, here) are counted within each grid cell at each time. The cells containing notifications are thus considered as sensible pseudo-receptors for the release of the Lagrangian particles in backward stochastic trajectories. In the second case a cluster analysis based on spatial coordinates is applied at each time interval. To establish the clustering level, a spatial scale of 500-m radius and a variable minimum number of alerts per cluster are considered. In the present application, the minimum number of alerts per cluster may vary from 3 to 10 depending on the maximum number of citizen notifications received at each time interval. The cluster centroids are assigned as the location of the pseudo-receptors and used as retro-emission sources in the backward RetroSPRAY simulation.

In Fig. 3 a temporal sequence of the identified pseudo-receptors, from 0630 to 0900 UTC every 30 min, is shown to compare the two aggregation methods for the Case 20200413. This highlights the similarity and difference between the two aggregation methods in time and space. In Fig. 4, the final spatial locations of pseudo-receptors are shown. With the grid-aggregation, only 5 cells act as pseudo-receptors, defining a total of 14 pseudo-observations in time. In fact, while their locations are the same at all times, the emission from the single cell may occur multiple times, in every sub-period when a sufficient number of alerts falls within the grid cell. Instead, in the second method the cluster centroids are recalculated at each time, therefore their locations differ at different times, even if they may happen to be close to each other. As a result, in this case 12 pseudo-observations are defined within the entire time period of the event, each at a different location.

The criteria applied to select the notifications and determine the pseudo-receptors, with their related pseudo-observations, have been established after a thorough examination of the effect of the values adopted for the thresholds and for the spatial scale used in grouping or clustering. The final choice resulted to be applicable to all three case studies here considered. Clearly, such criteria may still be subject to changes depending on the specific conditions characterising the nuisance event. For instance, a lower number of notifications might be expected when the episode occurs in the night, or whenever the citizens might be unable or get disaffected to the alerting duties.

The choice of the grid origin, i. e. the centre coordinates of the most South-Western gridbox, is arbitrary, and may affect the grid aggregation. This makes the clustering method more objective and has lead us to choose clustering as the aggregation method for the results shown in this work — and for the operational implementation.

4.2. Elaboration of the output

The retro-puff fields are combined, through a process that calculates their geometric mean (Eqs. (1) and (3)) and their arithmetic mean (Eq. (2)), in order to build final maps describing the region where possible source can be potentially located. Further processing of this information enables associating a related probability map, identifying the areas corresponding to the four quartiles.

Space and time indexes are defined as follows.

- $i \equiv \langle i_x, i_y \rangle$ is a possible location, a grid point, of the forward source which is sought for: $i_x = 1 \ldots N_x$, $i_y = 1 \ldots N_y$, and $i = 1 \ldots I$ where $I = N_x N_y$;
- $n = 1 \ldots N$ is the time index of possible forward emissions;
- $j = 1 \ldots J$ is the time index of retro-emissions, i. e. of pseudo-observations;
- $k_j = 1 \ldots K_j$ is the index of retro-sources that actively emit at retro-emission time j: i. e. of pseudo-observation locations referred to time j.

Notice that both time indexes j and n increase forward in time. Clearly, a source can start emitting before the odour peak is perceived and alerts are sent. Therefore, the backward simulation starts at the last time j and goes backward a n_0 number of intervals *before* – forwardly speaking – the first pseudo-observation time $j = 1$. As a consequence, when both indexes n and j, which are independent of each other, refer to the same time interval, the following relationship holds between them: $n = j + n_0$.

The geometric mean (Eqs. (1) and (3)) is used as a logical "AND" because, being based on a point-by-point product of fields, its value is large where all averaged fields are large, and small when even one of them is small. It can also be seen as an "intersection" of fields.

Similarly, the arithmetic mean is used as a logical "OR", because, being based on a (point-by-point) sum of fields, its value is large where any of the averaged fields is large, and small only where all of them are small. It can be seen as a "union" of fields.

Retro-puff fields are combined by performing geometric means and arithmetic means in the following three steps.

1. The sought-for source must determine all pseudo-observations of each time j. A logical AND operator is then appropriate, and the geometric mean of all fields generated by retro-puffs emitted from different locations k_j, at the same retro-emission time j, is calculated for each possible forward emission time n and location i.

$$p(i,n,j) = \prod_{k_j=1}^{K_j} \chi\left(i,n,j,k_j\right)^{\frac{1}{K_j}} \tag{1}$$

where $\chi\left(i,n,j,k_j\right)$ is the field of a retro-puff emitted at time j from location k_j and evaluated at time n in every gridpoint i, as calculated by RetroSPRAY. The resulting p array has then three indexes: i, n, j.

It is appropriate to keep separated, for the moment, pseudo-observations referred to different times j; they are combined together later, at the third stage described below. The reason is explained right after Eq. (4).

Fig. 5 shows two examples of geometric mean of retro-puff fields referred to the Case 20200413 (discussed in Section 5.1). The retro-puffs have all been emitted in the interval 0730–0700 from four different locations (i. e. citizen alert cluster centres), respectively reported in

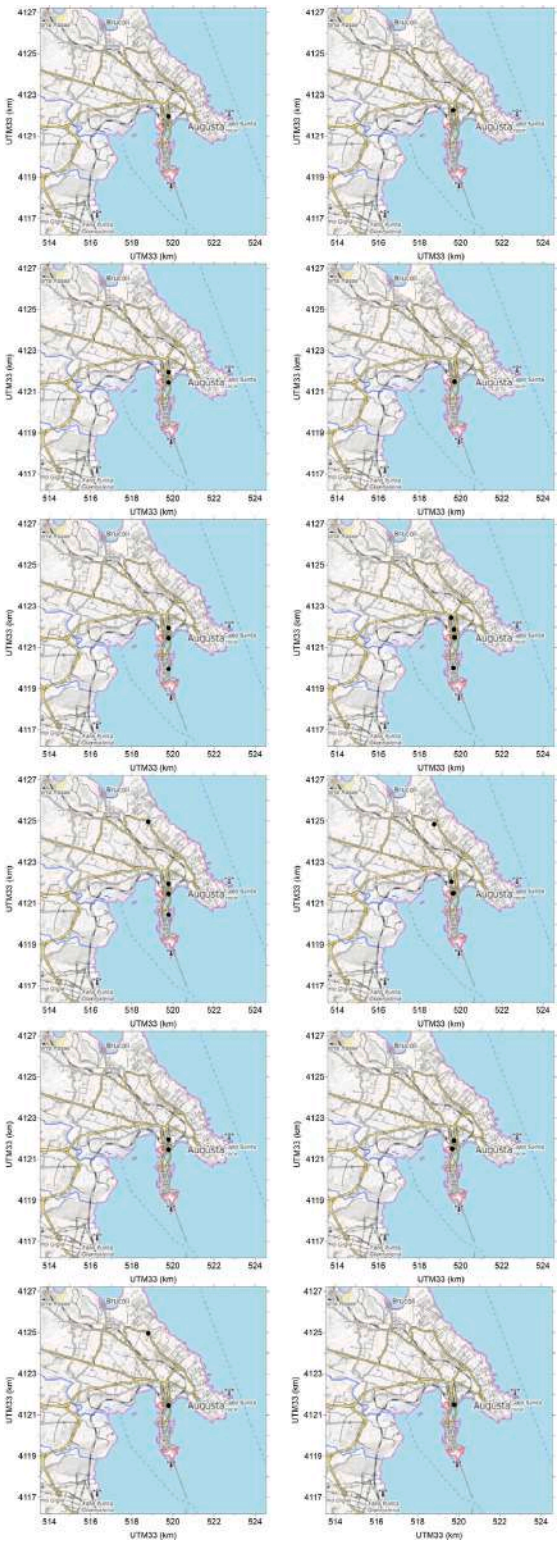

Fig. 3. Case 20200413. Area inside the black square in Fig. 1. Comparison between the locations of the pseudo-observations identified through the grid (left) and cluster (right) methods for six 30-minutes time intervals, from 0600–0630 (top) to 0830–0900 (bottom) UTC.

frames (a) and (e), (b) and (f), (c) and (g), (d) and (i). The four retro-puff fields from (a) to (d) are evaluated in the interval 0700–0630, the four fields from (e) to (h) in the interval 0600–0530: the retro-puffs of these last have then evolved for a longer backward time. It should be remembered that these evaluation intervals are times (n index) of possible forward emission from the sought-for source. In the right column, the field in (B) frame is the geometric mean of the four (a)–(d) retro-puff fields and the field in (D) frame is the geometric mean of the other four ones, (e)–(h). As it can be seen, the shaded area in geometric mean is common to the four retro-puff fields: the geometric mean field can be interpreted as an intersection of possible source locations, or a logical AND among the four logical conditions represented by the retro-puff fields.

2. The sought-for source can determine the pseudo-observations of time j by emitting at any (one or another) time $n \leq j$. For each retro-emission time j, the arithmetic mean (i.e. logical OR) on all possible forward emission times $n \leq j$ is then calculated:

$$s(i,j) = \sum_{n=1}^{j} \frac{1}{j} p(i,n,j) \tag{2}$$

The resulting array s has two indexes: i, j. Fig. 6 shows an example of such an arithmetic mean. All retro-puffs involved in this figure have been emitted in the same interval, 0730–0700, from four different locations (the same cluster centres of Fig. 5). The seven geometric means shown in panels from (A) to (G) have been calculated each at a different backward evolution interval, from 0730–0700 to 0430–0400. The field in panel (δ) is their arithmetic mean and it can be seen as the "union" of the geometric means, i. e. as an OR operator: it is large where one or another of the geometric mean fields is large.

3. The sought-for source must determine all pseudo-observations, referred to any time j. The geometric mean (i.e. logical AND) on all retro-emission times j is then calculated:

$$c(i) = \prod_{j=1}^{J} s(i,j)^{\frac{1}{J}} \tag{3}$$

The resulting array c only depends on the spatial location (grid) index $i \equiv \langle i_x, i_y \rangle$: it is a field that can be shown as a map.

The sequence order of geometric and arithmetic mean operations in the resulting field is relevant. In fact, by substituting Eqs. (1) and (2) in Eq. (3), one obtains:

$$c(i) = \prod_{j=1}^{J} \left\{ \sum_{n=1}^{j} \frac{1}{j} \left[\prod_{k_j=1}^{K_j} \chi\left(i,n,j,k_j\right)^{\frac{1}{K_j}} \right] \right\}^{\frac{1}{J}} \tag{4}$$

Choosing a different operation sequence would imply unwanted constraints, such as, for example, that every forward time n should forcefully be implied in pseudo-observations taken at all times j.

Fig. 7 shows all arithmetic means of geometric means of fields generated by retro-puffs emitted all along the time period when alert clusters have been defined, from 0900 to 0600. Their geometric mean is the third – and final – step of RetroSPRAY output elaboration, the Possible Source Location (PSL) field shown in Fig. 8a. Remark that the area covered by this final field has a much smaller extension than each of the arithmetic means of Fig. 7: in fact this is the area which is common to all of them.

The final field obtained is the PSL field and shows the possible locations of the sought-for source. This map, shown for the three cases in panel (a) of Figs. 8, 11 and 13, should be interpreted in the following way. In a possible SPRAY forward integration, a plume emitted from a source located where the PSL has a large value, i.e. at grid-boxes that are coloured with darker tones, would directly hit the alert areas, where the pseudo-observations are located. Usually, a comparatively small amount of emitted mass is sufficient to "explain" the pseudo-observations in such cases. On the contrary, a forward plume emitted from a source located at grid-boxes where the PSL is small (but nonzero) would hit the alert areas only marginally, and a much larger amount of emitted mass would be necessary to "explain" the pseudo-observations; moreover other areas, where no alert had been recorded, would also be hit. Finally, in a forward SPRAY simulation, a source

Fig. 4. Case 20200413. Area inside the black square in Fig. 1. Comparison between the locations of the pseudo-observations identified through the grid (a) and cluster (b) methods for the entire retro-emission period, 0900–0600 UTC. The pseudo-observations distribute in 6 time intervals (Fig. 3) and they are 14 at 5 locations for the grid method, 12 at 12 different locations for the cluster method.

Table 1
Time periods of the backward simulation and of the emissions for the three case studies and coordinates of the receptors from which the retro-puffs are released.

	Backward simulation time period (UTC)		Emission time period (UTC)		Retro-release coordinates (UTM m)	
	Start	End	Start	End	X	Y
13/04/2020	09:00	04:00	09:00	08:30	519784	4121497
			08:30	08:00	519591	4121504
			08:30	08:00	519674	4121896
			08:00	07:30	519556	4122052
			08:00	07:30	519636	4121484
			08:00	07:30	518708	4124853
			07:30	07:00	519646	4120010
			07:30	07:00	519702	4121491
			07:30	07:00	519674	4121878
			07:30	07:00	519535	4122447
			07:00	06:30	519703	4121488
			06:30	06:00	519639	4122255
03/04/2020	21:30	17:30	21:30	21:00	511356	4114978
			21:00	20:30	511732	4114609
			20:30	20:00	511316	4114518
			20:00	19:30	511315	4114698
01/04/2020	15:00	10:30	15:00	14:30	511136	4114748
			14:30	14:00	511074	4114748
			14:30	14:00	512596	4114445
			14:00	13:30	511132	4114598
			13:30	13:00	511027	4114842
			13:30	13:00	511684	4114596
			13:00	12:30	511235	4114571

located at grid-boxes where the PSL is zero would not reach the alert areas at all: it would go elsewhere.

When a similar elaboration is applied to proper observations, i. e. measured pollutant concentrations (Tinarelli et al., 2018), an important information is given by observations of small concentration values: ideally zero, or background-level concentration. Such observations state that at their times and locations the concentration peak under study is not present. This information can be used to reject impossible source location and emission times, that would have otherwise determined high concentration values at those locations and times. Such a rejection information is not available when, in place of proper quantitative observations, pseudo-observations are built by aggregating alerts provided by untrained citizens on a voluntary basis. This means that we do not have the possibility of imposing a further selection on locations shown in the PSL maps. In particular, the highest PSL values may result to be placed very close to the denser alert area, even if the real source is located upstream.

The PSL field is non-dimensional, and its value may depend on the number of pseudo-observations and of aggregated alerts. From the PSL field, though, it is easy to build an information that enables a comparison between different cases and that, at the same time, represents an information that may be more understandable by a final user. We recall that each retro-puff is composed by Lagrangian particles, whose collection intrinsically represents a statistical ensemble. The combination of retro-puff fields obtained by the described AND and OR logical operators is the synthetic PSL field which, appropriately normalised, leads to define a probability density function in space. In fact, the ratio of the PSL field to its total sum at all grid points can be interpreted as a spatial, two-dimensional, probability density function (SPDF). The map in panel (b) of Fig. 8, Figs. 11 and 13 shows the SPDF, where the coloured zones are separated by the probability density levels Q1, Q2 and Q3. These last are chosen so that, in every map, each zone amounts for 25 % probability, with highest SPDF values in the darkest zone and smallest positive SPDF values in the lightest

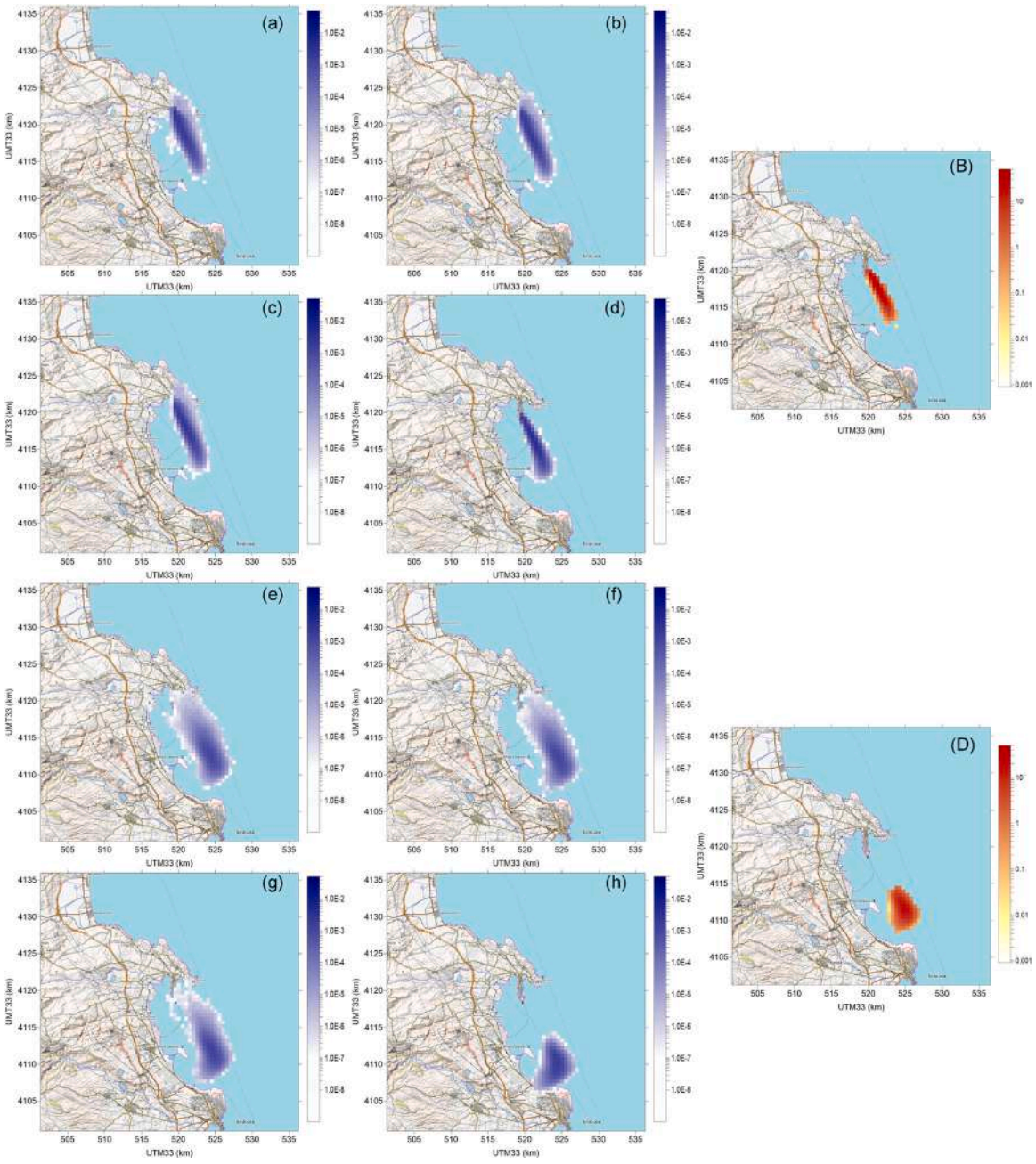

Fig. 5. Case 20200413. Area inside the red square in Fig. 1. First step of RetroSPRAY output elaboration: example of geometric mean of retro-puffs fields. The plots show the backward evolution of retro-puffs emitted from four different locations (a–e, b–f, c–g and d–h) in the interval 0730-0700, plotted respectively at 0700-0630 interval for panels (a) to (d), and at 06:00-0530 interval for panels (e) to (h). In frames (B) and (D) the fields of the geometric means of the retro-puff fields from (a) to (d) and from (e) to (h) are reported, respectively.

coloured zone. This means that the source is expected to lie within any of the four coloured zones with 100 % probability, within all but the lightest coloured zone (> Q1) with 75 % probability, within any of the two darkest zones (> Q2) with 50 % probability, and within the single darkest zone (> Q3) with 25 % probability. Notice that the darkest zone is the smallest: this is where SPDF values are higher, namely where probability is denser. Consequently, the probability that the source lies within a "unit" area is higher if this is located inside the darkest zone than elsewhere.

5. Results of simulations for real cases in the frame of the NOSE project

For each of the three case studies SMART simulations were run having available the MOLOCH-ARAMIS meteorological fields at 0.5 km grid resolution, nested in the GFS (Global Forecast System model) data, for the full day and ending the RetroSPRAY backward simulation a couple of hours before the start of the event. In Table 1 the details of the 30-minutes retro-emissions from the clustered pseudo-observations locations are reported for the three case studies.

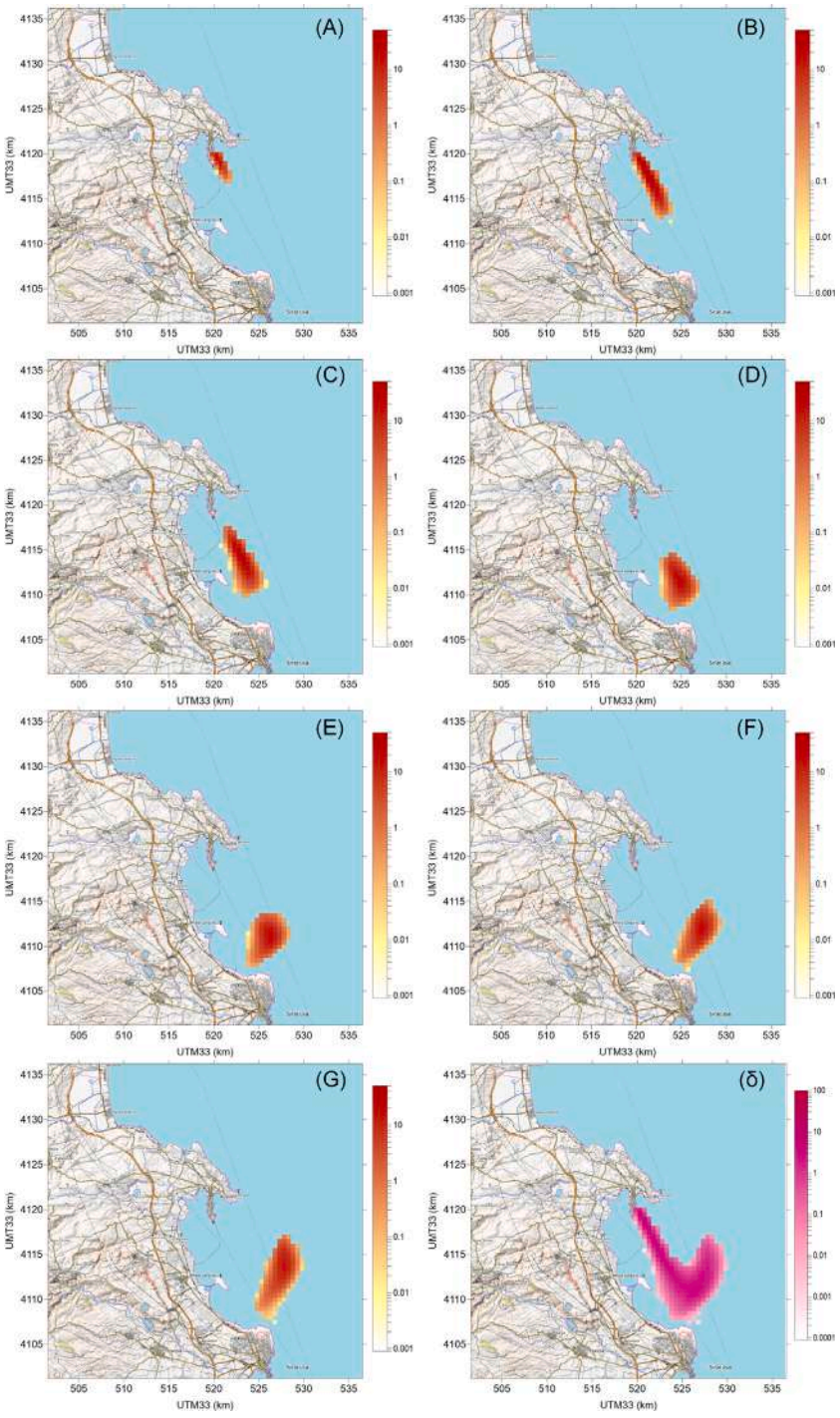

Fig. 6. Case 20200413. Area inside the red square in Fig. 1. Second step of RetroSPRAY output elaboration: example of the arithmetic mean of geometric means of retro-puff fields. All retro-puffs, from which this figure is generated, were emitted in the same interval, 0730–0700. The seven geometric means, from (A) to (G), have been calculated each at a different backward evolution time interval, from 0730–0700 to 0430–0400. The plot in frame (δ) is their arithmetic mean.

We remark that the RetroSPRAY time-backward integration is set up to generate retro-puffs, not retro-plumes. This means that all retro-puffs evolve separately. A single retro-puff is emitted from the location and time of each pseudo-observation, and retro-puff fields are not added or otherwise combined during a RetroSPRAY integration. Even when the grid aggregation (see Section 4.1) is used and several pseudo-observations may have the same location (but different times), their emitted retro-puffs are kept separated during the time-backward evolution. Retro-puff fields are combined after the RetroSPRAY simulation, using the three-step elaboration described in Section 4.2

5.1. Case 20200413

On April 13, 2020, a large number of notifications were received, as described in Section 3. The circulation in the area of Augusta is characterised by a weak vortex in the first hours of the period considered, starting at 0400 UTC, which then moves north-eastward till vanishing. In the following hours, from 0600 UTC a south-westerly flow develops and reinforces, with wind speed increasing in time. The development of the wind field in the area can be seen in the Animation_WindField_13042020.gif file supplied in the Supplementary

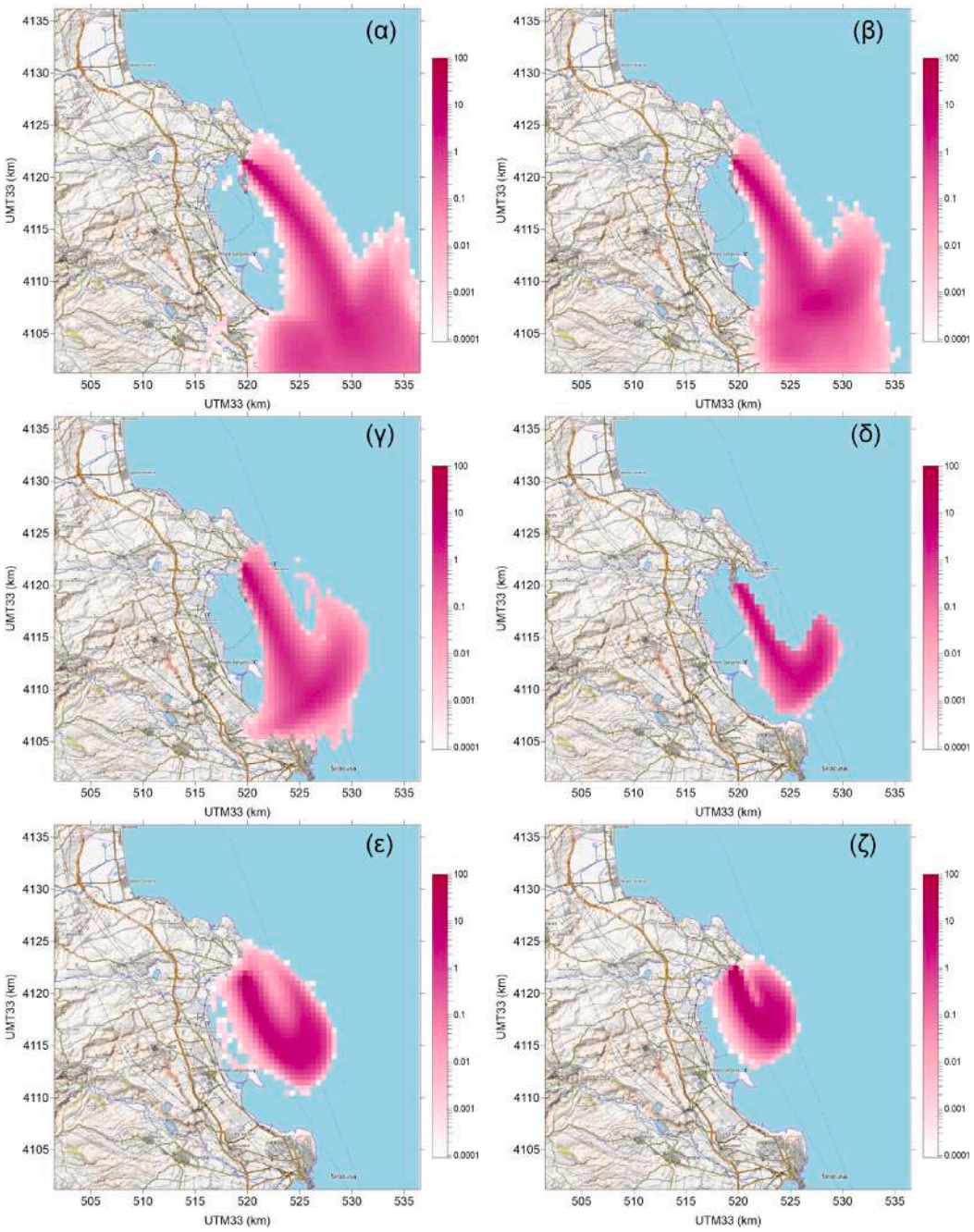

Fig. 7. Case 20200413. Area inside the red square in Fig. 1. Arithmetic means obtained by combining the fields from retro-puffs emitted at the six intervals with retro-emission from 0900–0830 to 0630–0600. The field in (δ) panel (interval 0730-0700) is the same shown in Fig. 6. The geometric mean of these fields, shown in Fig. 8a, is the third step of RetroSPRAY output elaboration.

Material. With RetroSPRAY model, twelve 30-minutes releases were simulated backward in time from the cluster centroids, following their dispersion from 0900 to 0400 UTC, as detailed in Table 1. Fig. 8a shows the PSL map. Thanks to the high number of alerts, the possible areas of provenience result to be rather well defined based on the applied post-processing methodology. This reflects also in the SPDF map, in Fig. 8b, where the most probable sub-areas are clearly identified.

In order to check whether the outputs obtained applying the newly developed methodology are reliable, a forward simulation was performed with SPRAY dispersion model. The potential source was located in one of the most probable sub-areas, considering a continuous point release in the location of UTM coordinates in metres (X,Y)=(520791,4119959). The test is qualitative and aimed at verifying if a plume released from such source is effectively hitting the receptors in due time. Therefore, the interest here is to reproduce the distribution of the tracer in space as impacted areas, and no quantitative evaluation of the actual concentration is considered. In Fig. 9 the concentration maps are reported from 0500 UTC to 0900 UTC every 30 min (an animation for the full simulation period and time intervals is available in the Supplementary Material, file Animation_conc_13042020.gif). Just as reference for the scale of the concentration values, we cite that the emission was corresponding to 10^9 μg of Benzene every hour. The plume clearly covers the area from where the notifications were received and it is found to reach the different pseudo-receptors at the correct times. In Fig. 10 the map of the concentration averaged over the period between 0600 UTC and 0900 UTC, corresponding to the peak of notifications, is shown to provide an integrate view of the spatial distribution of the tracer. The results obtained by the forward

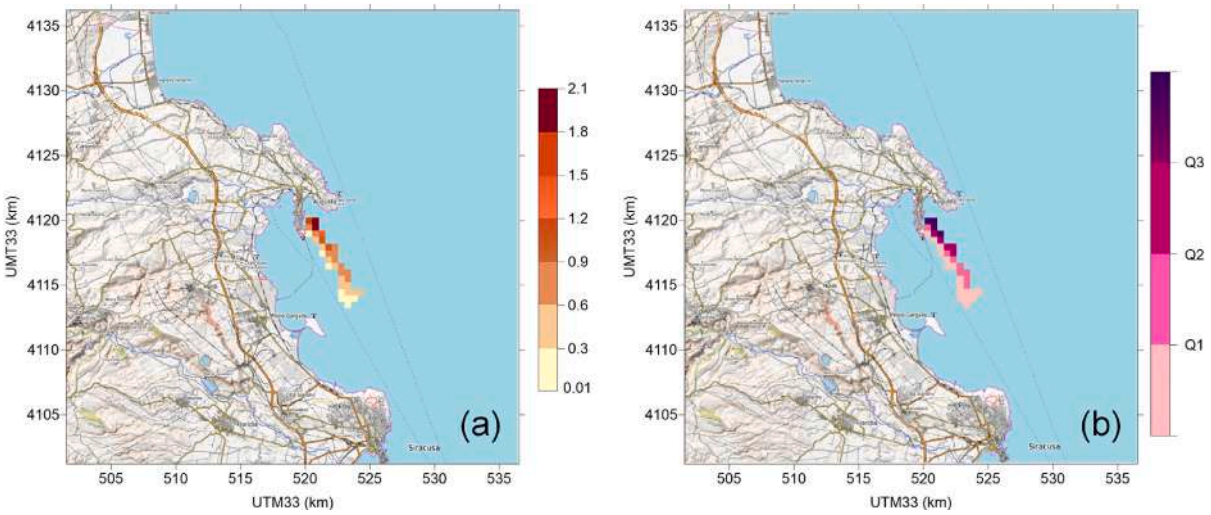

Fig. 8. Case 20200413. Area inside the red square in Fig. 1. Maps identifying (a) the area where potential sources may be located; (b) the related spatial probability density function (SPDF). The explict values of Q1, Q2, Q3 are not informative; their values are chosen so that each of the 4 shaded areas represent 25 % probability; moreover, since Q1 < Q2 < Q3, the darkest area encloses the highest values of the SPDF.

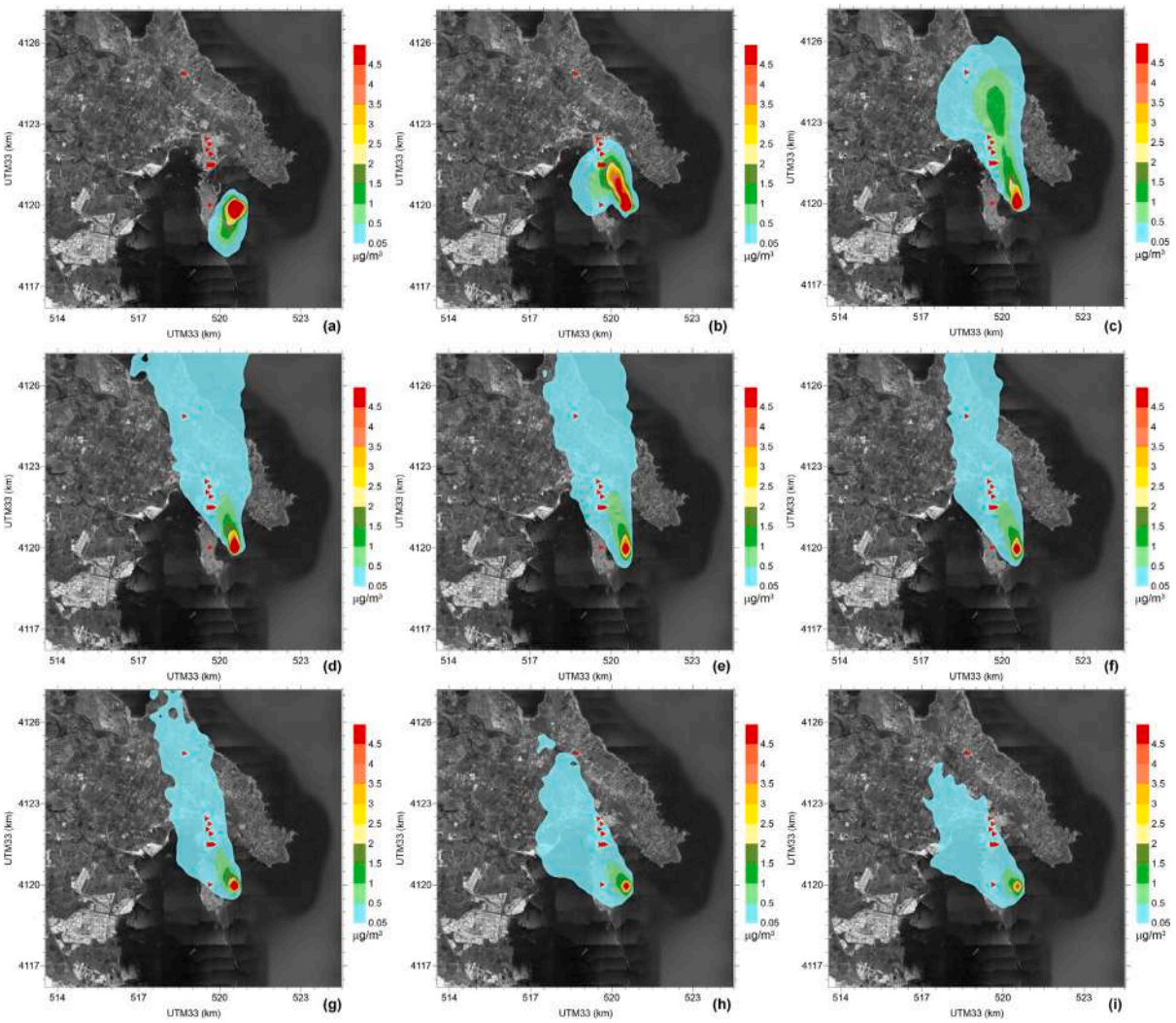

Fig. 9. Case 20200413. Area inside the black square in Fig. 1. SPRAY forward simulation, source (X,Y)=(520791,4119959) UTM (m). Maps of concentration from 0500 UTC (a) to 09:00 (i) UTC every 30 min. The red triangles indicate the locations of the receptors, corresponding to the clustered retro-sources in the RetroSPRAY backward simulation (see also the file Animation_conc_13042020.gif in the Supplementary Material).

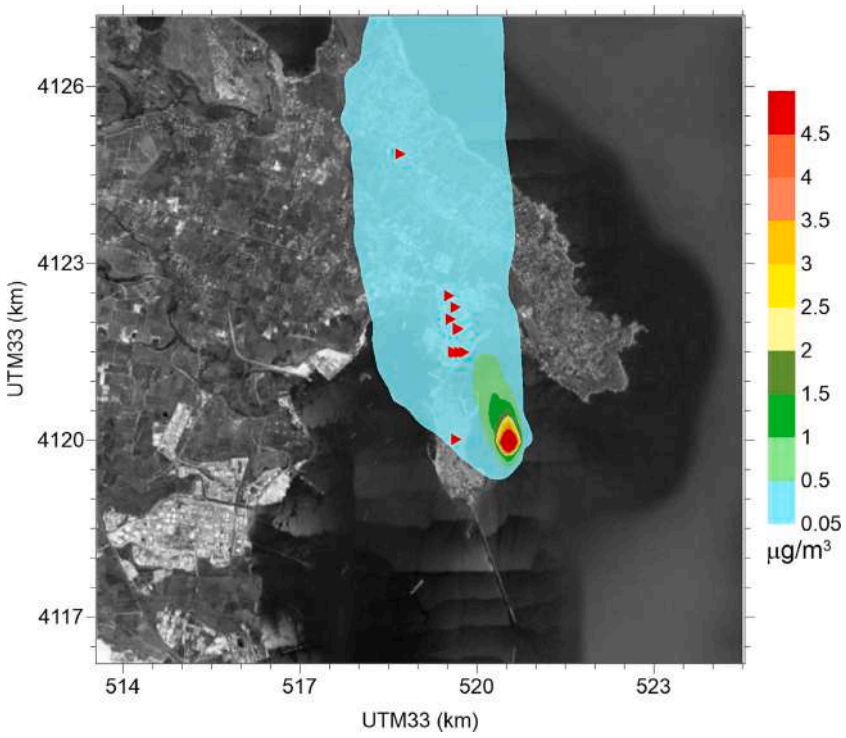

Fig. 10. Case 20200413. Area inside the black square in Fig. 1. SPRAY forward simulation, source (x,y)=(520791,4119959) UTM (m). Maps of concentration averaged over the period from 0600 UTC to 09:00 UTC. As in Fig. 9, the red triangles indicate the locations of the receptors, corresponding to the clustered retro-sources in the RetroSPRAY backward simulation.

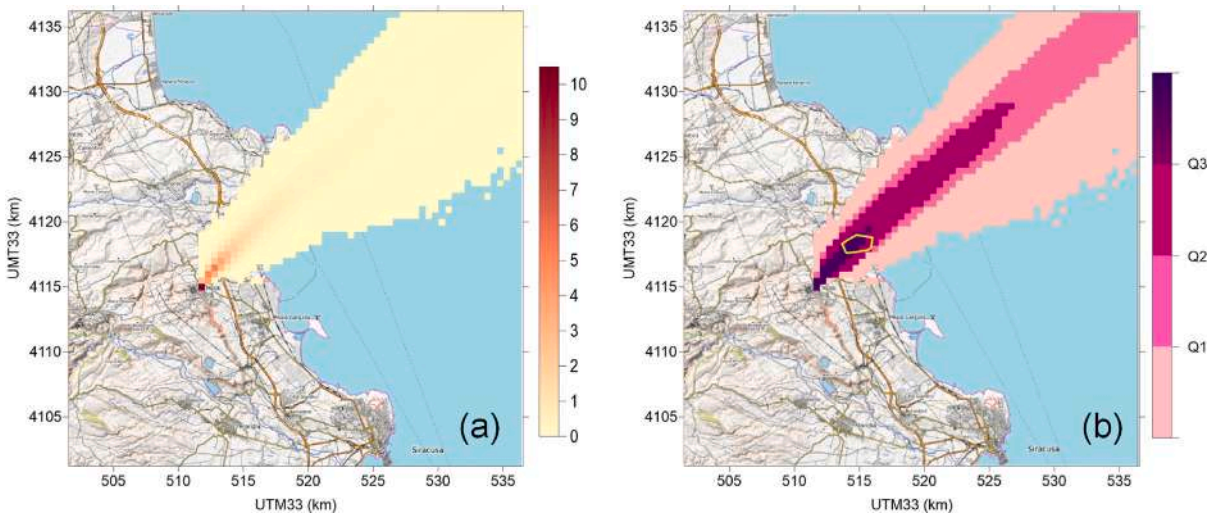

Fig. 11. Case 20200403. Area inside the red square in Fig. 1. Maps identifying: (a) the area where potential sources may be located; (b) the related SPDF as in Fig. 8, with a yellow polygon showing the verified source area.

simulation confirms that the application of the methodology provides a reliable assessment and definition of the potential odour sources.

5.2. Case 20200403

In this case the notifications were received mostly from the town of Melilli, then the source of the nuisance was identified in the industrial area north-east of the city after a field monitoring by ARPA Sicilia (see https://www.arpa.sicilia.it/picco-di-segnalazioni-di-cattivi-odori-a-melilli-sr-risultati-campionamenti-e-controlli/). During the peak of the event, between 1820 and 2120 UTC, a strong north-easterly wind was blowing over the area, with high speed as illustrated in the file Animation_WindField_03042020.gif (see the Supplementary Material). Four 30-minutes releases were simulated with RetroSPRAY model, as reported in Table 1. The PSL and SPDF maps in Fig. 11 show a larger spread of the area related to the lowest probability for the source location, as it can be expected given the low number of alerts used, leading to a lower level of selection in the methodology. At the same time, the area related to the highest probability, the fourth quartile, that is > 0.75 quantile, is captured in a well defined way and falls in the area where the industrial plant originating the odour nuisance is actually located, as highlighted in Fig. 11b. Also in this case, the proposed methodology is successful in detecting the area of provenience of the odour.

It can be seen that the highest probability zone (the darkest fourth quartile) extends downwind towards the area from where most notifications have been received. In this case, only four pseudo-observations

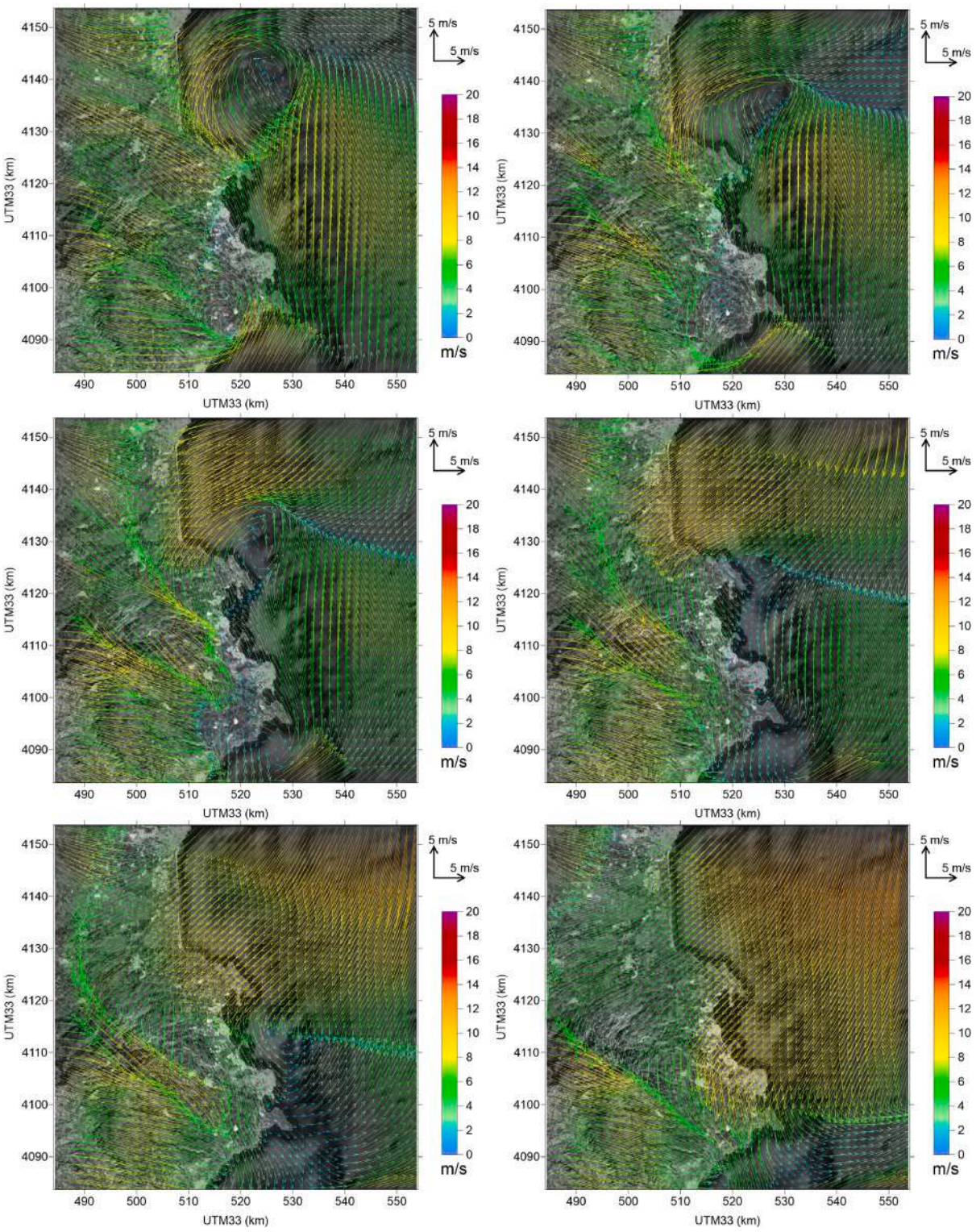

Fig. 12. Case 20200401. Maps at first model level (33-m height) of the wind velocity over the area from 1230 UTC (a) to 1500 UTC (f) every 30 minutes.

could be defined, and they are located very close to each other. This implies that a possible source could be located very close to (all of) them, which is quite typical when the notifications tend to concentrate in a small area, originating close cluster centroids. Such configuration does not allow a fine selection, which instead is effective when notifications are more distributed in space. This occurs in Case 20200413 (Section 5.1), where more pseudo-observations (i. e. retro-emissions) are available, spread on a wider area (Fig. 4b). Thus, accounting for all of them reduces the most probable source locations in an area farther away (Fig. 8b).

5.3. Case 20200401

This case study is characterised by a high uncertainty. The notifications are rather sparse in the area, arriving from Augusta, Siracusa, Priolo and with a peak from Melilli, thus generating 'spotted' signals.

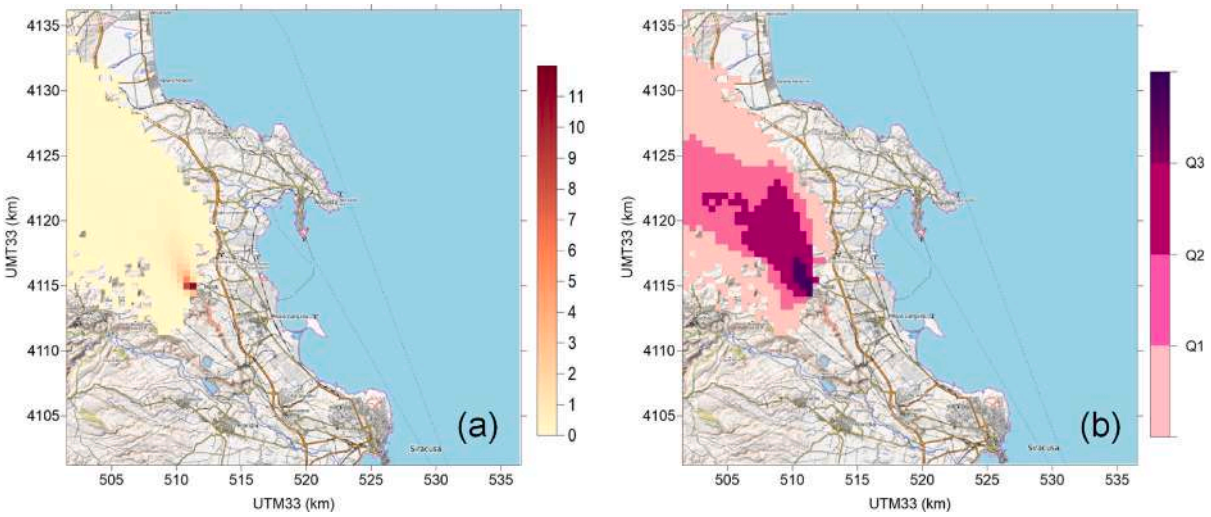

Fig. 13. Case 20200401. Area inside the red square in Fig. 1. Maps identifying (a) the area where potential sources may be located; (b) the related SPDF as in Figs. 8 and 11.

The spatial variability of the notifications indicate that the nuisance event affected a large area and may be connected with sharp changes in the wind regime over it. In Fig. 12 a sequence every 30 min of maps of the wind field at the first model level (33-m height) is reported from 1230 to 1500 UTC, the time period when the number of alerts is higher (in the file Animation_WindField_01042020.gif the maps are reported every 15 min, see the Supplementary Material). The maps show a very complex low level circulation associated to the passage of a cold front over the area. In the beginning, over the sea in the south-east sector, the wind tends to blow towards north-north-east, while in the north-east sector it blows westward. Over the land, the wind blows towards south-east or even eastward in the southern part of the domain. This gives rise to vortexes and re-circulations along the coast, which later on tend to break. In the end of the period, two dominant circulations establish, north-easterly on the sea towards land and north-westerly in the south part over land. Such a challenging condition has been chosen to address possible criticality in the proposed approach.

Seven 30-minutes releases were simulated with the RetroSPRAY model, as in Table 1. The relative large spread revealed by the PSL and SPDF maps in Fig. 13 is reflecting the variability and uncertainty of the case study. Yet, the quantiles of higher probability allow identifying a restricted potential areas of provenience of the odour nuisance, west and north-west of Melilli. Samplings with a canister were performed in the town of Melilli and analysed by ARPA Sicilia, revealing the presence of VOCs, with relatively high values of benzene, toluene, etilbenzene, e p-m-o-xilene. The analysis confirmed that the area around Melilli was the most impacted by the event, even if the potential source remained unknown. In such uncertain situation, the SMART modelling outcome together with the methodology for its elaboration can play a decisive role in supporting and driving the field measurements and the investigation aimed at identifying the potential source. Also in this case, it has been possible to provide a rather clear indication of the potential location of the release.

6. Conclusions

The novel and original approach developed to (i) use citizens' notifications as input to the Lagrangian particle dispersion model SPRAY, in its backward-mode version RetroSPRAY, and to (ii) elaborate the simulation output of SMART modelling system to trace the potential source of odour nuisance, demonstrated to be reliable, promising and applicable. A quantitative information based on probability density maps could be processed and made available as final outcome of the methodology.

In all three selected case studies, corresponding to events notified through the Web-App NOSE in April 2020 and characterised by rather different conditions, it was possible to obtain a clear indication of the most probable area of provenience of the odour emission, thus locating the potential sources. The verification of the results was feasible in the events of April 13 2020, by performing forward simulations with SPRAY model, and April 3 2020, when the source of release was identified thanks to field measurements carried out during the event itself. The third case, on April 1 2020, had few alerts, sparse in space and erratic in time. It was a critical episode, during which the flow circulation was very complex and variable and a large area was affected by the odour nuisance. Correspondingly, the uncertainty in identifying the possible source location could just be very high. Also in this case, the methodology was able to tighten the most probable areas of release, providing a rather clear indication of the potential provenience zone.

Further developments may be considered to reduce or overcome the uncertainty that can affect the most critical cases, like those with too few and/or too sparse notifications. They are related to the use of zero values for the (pseudo)observations, as it can be done in air pollution modelling when concentration measurements are available (Tinarelli et al., 2018). Zero-values can be used to exclude areas where concentrations of the tracer of interest are not detected. However, in case of using citizen notifications, this would imply to organise a net of "observers" who should be informed of the event in course in the area and should notify whether no nuisance is perceived in their location. Such strategy can be a future challenge for the NOSE Project, and the methodology here proposed could be rather easily adapted to include and treat such additional information.

Indeed, having a high number of notifications allows optimising and maximising the efficacy of the methodology. Therefore, the contribution of the citizens and their direct involvement should be promoted and encouraged, pursuing the highest benefit from the citizen-science approach.

The use of a meteo-dispersive system represents an advancement with respect to consider deterministic trajectories, because also the turbulent features of the atmospheric flow are accounted for and represented. At present, the operational version of the full system, integrating SMART modelling suite in NOSE Web-App, has been implemented and will be applied for future odour nuisance events in the area of Siracusa Province in Sicily (Italy). The system can be efficiently implemented for any areas in the Italian territory which can be sensible to noxious odour releases, to its impact on the population and related exposure. The identification of the possible source area allows the officers of the Regional Environmental Agencies (ARPA Sicilia, in the

present case) to possibly perform dedicated monitoring and measurements in that area during and after the event, considering also the known potential emitting sources. Then, when they are able to identify the plant releasing the substances causing the odour nuisance, they can intervene by imposing measures to contain odorous emissions.

We underline that, even if the approach was developed for a modelling suite interfacing a meteorological model with a Lagrangian particle dispersion model, the various modules for the elaboration of the input and output are independent, the complete system is handled by scripts that can be adapted to other types of model configuration. Thus, the methodology developed for the inputs and outputs can be integrated with any other system where retro-puffs are produced or by running an adjoint version of a Eulerian model.

CRediT authorship contribution statement

Silvia Trini Castelli: Conceptualization, Methodology, Software, Validation, Investigation, Resources, Supervision, Writing – original draft, Writing – review & editing, Visualization. **Francesco Uboldi:** Conceptualization, Methodology, Software, Validation, Investigation, Formal analysis, Writing – original draft, Writing – review & editing, Visualization. **Gianni Luigi Tinarelli:** Conceptualization, Methodology, Software, Validation, Investigation, Writing – original draft, Writing – review & editing, Visualization. **Oxana Drofa:** Methodology, Software, Resources, Data curation. **Piero Malguzzi:** Conceptualization, Methodology, Software, Investigation, Resources. **Paolo Bonasoni:** Resources, Writing – review & editing, Supervision, Project administration, Funding acquisition.

Declaration of competing interest

The authors declare that they have no known competing financial interests or personal relationships that could have appeared to influence the work reported in this paper.

Data availability

Data will be made available on request.

Acknowledgements

The authors like to thank Giorgio Resci, of INKODE Company, and Tony C. Landi, CNR-ISAC Bologna, for their support in integrating SMART modelling system in NOSE Web-App, Vincenzo Infantino and Anna Abita from ARPA Sicilia for the great support provided under the NOSE project. The development of the new methodology and the SMART simulations were performed while Francesco Uboldi was working for ARIANET Srl, Milan.

Appendix A. Supplementary data

Supplementary material related to this article can be found online at https://doi.org/10.1016/j.atmosenv.2023.119992.

References

Anfossi, D., Alessandrini, S., Trini Castelli, S., Ferrero, E., Oettl, D., Degrazia, G., 2006. Tracer dispersion simulation in low wind speed conditions with a new 2D langevin equation system. Atmos. Environ. 40, 7234–7245. http://dx.doi.org/10.1016/j.atmosenv.2006.05.081.

Anfossi, D., Tinarelli, G., Trini Castelli, S., Nibart, M., Olry, C., Commanay, J., 2010. A new Lagrangian particle model for the simulation of dense gas dispersion. Atmos. Environ. 44, 753–762. http://dx.doi.org/10.1016/j.atmosenv.2009.11.041.

Armand, P., Olry, C., Albergel, A., Duchenne, C., Moussafir, J., 2013. H15-37: Development and application of Retro-SPRAY, a backward atmospheric transport and dispersion model at the regional and urban scale. In: Proceedings of the 15th International Conference on Harmonisation Within Atmospheric Dispersion Modelling for Regulatory Purposes. HARMO 2013, pp. 789–793.

Bergamaschi, P., Corazza, M., Karstens, U., Athanassiadou, M., Thompson, R.L., Pison, I., Manning, A.J., Bousquet, P., Segers, A., Vermeulen, A.T., Janssens-Maenhout, G., Schmidt, M., Ramonet, M., Meinhardt, F., Aalto, T., Haszpra, L., Moncrieff, J., Popa, M.E., Lowry, D., Steinbacher, M., Jordan, A., O'Doherty, S., Piacentino, S., Dlugokencky, E., 2015. Top-down estimates of European CH_4 and N_2O emissions based on four different inverse models. Atmos. Chem. Phys. 15, 715–736. http://dx.doi.org/10.5194/acp-15-715-2015, URL: https://acp.copernicus.org/articles/15/715/2015.

Bisignano, A., Trini Castelli, S., 2018. Development of the SMART (Spray-Moloch Atmospheric Regional Tool) Modelling System: The ARAMIS Interfacing Module. Technical Report. ISAC-TO/01-2018.

Bisignano, A., Trini Castelli, S., 2021. SMART modeling suite: Assessment of the turbulence parameterisation for the simulation of atmospheric circulation and dispersion. In: Mensink, C., Matthias, V. (Eds.), Air Pollution Modeling and Its Application XXVII. Springer Berlin Heidelberg, Berlin, Heidelberg, pp. 101–106. http://dx.doi.org/10.1007/978-3-662-63760-9_15.

Bisignano, A., Trini Castelli, S., Malguzzi, P., 2020. Development and verification of a new meteo-dispersive modelling system for accidental releases in the Italian territory: SMART. In: Mensink, C., Gong, W., Hakami, A. (Eds.), Air Pollution Modeling and Its Application XXVI. Springer International Publishing, Cham, pp. 77–81. http://dx.doi.org/10.1007/978-3-030-22055-6_13.

Buzzi, A., Davolio, S., D'Isidoro, M., Malguzzi, P., 2004. The impact of resolution and of MAP reanalysis on the simulations of heavy precipitation during MAP cases. Meteorol. Z. 13, 91–97. http://dx.doi.org/10.1127/0941-2948/2004/0013-0091.

Buzzi, A., Fantini, M., Malguzzi, P., Nerozzi, F., 1994. Validation of a limited-area model in cases of mediterranean cyclogenesis – surface fields and precipitation scores. Meteorol. Atmos. Phys. 53, 137–153. http://dx.doi.org/10.1007/BF01029609.

Carvalho, J., Anfossi, D., Castelli, S., Degrazia, G., 2002. Application of a model system for the study of transport and diffusion in complex terrain to the TRACT experiment. Atmos. Environ. 36, 1147–1161. http://dx.doi.org/10.1016/S1352-2310(01)00559-3.

Chiapello, I., Bergametti, G., Chatenet, B., Bousquet, P., Dulac, F., Soares, E., 1997. Origins of African dust transported over the northeastern tropical Atlantic. J. Geophys. Res.: Atmos. 102, 13701–13709. http://dx.doi.org/10.1029/97JD00259.

Elbern, H., Strunk, A., Schmidt, H., Talagrand, O., 2007. Emission rate and chemical state estimation by 4-dimensional variational inversion. Atmos. Chem. Phys. 7, 3749–3769. http://dx.doi.org/10.5194/acp-7-3749-2007.

Ferrarese, S., Trini Castelli, S., 2019. Detection of CO2 source areas using two Lagrangian particle dispersion models, at regional scale and long range. In: Proceedings of the 19st International Conference on Harmonisation Within Atmospheric Dispersion Modelling for Regulatory Purposes. HARMO 2019, p. 5.

Flesch, T., Wilson, J., Yee, E., 1995. Backward-time Lagrangian stochastic dispersion models and their application to estimate gaseous emissions. J. Appl. Meteorol. 34, 1320–1332. http://dx.doi.org/10.1175/1520-0450(1995)034<1320:BTLSDM>2.0.CO;2.

Gurney, K., Law, R., Denning, A., Rayner, P., Baker, D., Bousquet, P., Bruhwiler, L., Chen, Y., Ciais, P., Fan, S., Fung, I., Gloor, M., Heimann, M., Higuchi, K., John, J., Maki, T., Maksyutov, S., Masarie, K., Peylin, P., Prather, M., Pak, B., Randerson, J., Sarmiento, J., Taguchi, S., Takahashi, T., Yuen, C., 2002. Towards robust regional estimates of CO2 sources and sinks using atmospheric transport models. Nature 415, 626–630. http://dx.doi.org/10.1038/415626.

Hourdin, F., Talagrand, O., 2006. Eulerian backtracking of atmospheric tracers. I: Adjoint derivation and parametrization of subgrid-scale transport. Q. J. R. Meteorol. Soc. 132, 567–583. http://dx.doi.org/10.1256/qj.03.198.

Hutchinson, M., Oh, H., Chen, W.H., 2017. A review of source term estimation methods for atmospheric dispersion events using static or mobile sensors. Inf. Fusion 36, 130–148. http://dx.doi.org/10.1016/j.inffus.2016.11.010.A.

Kopacz, M., Jacob, D.J., Henze, D.K., Heald, C.L., Streets, D.G., Zhang, Q., 2009. Comparison of adjoint and analytical Bayesian inversion methods for constraining Asian sources of carbon monoxide using satellite (MOPITT) measurements of CO columns. J. Geophys. Res. - Atmos. 114, http://dx.doi.org/10.1029/2007JD009264.

Malguzzi, P., Buzzi, A., Drofa, O., 2011. The meteorological global model GLOBO at the ISAC-CNR of Italy assessment of 1.5 yr of experimental use for medium-range weather forecasts. Weather Forecast. 26, 1045–1055. http://dx.doi.org/10.1175/WAF-D-11-00027.1.

Malguzzi, P., Grossi, G., Buzzi, A., Ranzi, R., Buizza, R., 2006. The 1966 century flood in Italy: A meteorological and hydrological revisitation. J. Geophys. Res.: Atmos. 111, http://dx.doi.org/10.1029/2006JD007111.

Nanni, A., Tinarelli, G., Solisio, C., Pozzi, C., 2022. Comparison between puff and Lagrangian particle dispersion models at a complex and coastal site. Atmosphere 13, http://dx.doi.org/10.3390/atmos13040508.

Platt, N., DeRiggi, D., 2012. Comparative investigation of Source Term Estimation algorithms using FUSION field trial 2007 data: linear regression analysis. Int. J. Environ. Pollut. 48, 13–21. http://dx.doi.org/10.1504/IJEP.2012.049647, 13th International Conference on Harmonisation within Atmospheric Dispersion Modelling for Regulatory Purposes, Paris, France, Jun (2010) 01-05.

Pudykiewicz, J., 1998. Application of adjoint tracer transport equations for evaluating source parameters. Atmos. Environ. 32, 3039–3050. http://dx.doi.org/10.1016/S1352-2310(97)00480-9.

Rajaona, H., Septier, F., Armand, P., Delignon, Y., Olry, C., Albergel, A., Moussafir, J., 2015. An adaptive Bayesian inference algorithm to estimate the parameters of a hazardous atmospheric release. Atmos. Environ. 122, 748–762. http://dx.doi.org/10.1016/j.atmosenv.2015.10.026.

Schauberger, G., Piringer, M., Knauder, W., Petz, E., 2011. Odour emissions from a waste treatment plant using an inverse dispersion technique. Atmos. Environ. 45, 1639–1647. http://dx.doi.org/10.1016/j.atmosenv.2011.01.007.

Thompson, R.L., Ishijima, K., Saikawa, E., Corazza, M., Karstens, U., Patra, P.K., Bergamaschi, P., Chevallier, F., Dlugokencky, E., Prinn, R.G., Weiss, R.F., O'Doherty, S., Fraser, P.J., Steele, L.P., Krummel, P.B., Vermeulen, A., Tohjima, Y., Jordan, A., Haszpra, L., Steinbacher, M., Van der Laan, S., Aalto, T., Meinhardt, F., Popa, M.E., Moncrieff, J., Bousquet, P., 2014. TransCom N2O model inter-comparison - Part 2: Atmospheric inversion estimates of N2O emissions. Atmos. Chem. Phys. 14, 6177–6194. http://dx.doi.org/10.5194/acp-14-6177-2014.

Tinarelli, G., Anfossi, D., Bider, M., Ferrero, E., Trini Castelli, S., 2000. A new high performance version of the Lagrangian particle dispersion model spray, some case studies. In: Gryning, S., Batchvarova, E. (Eds.), Air Pollution Modeling and Its Application XIII. Springer, Boston, MA, USA, pp. 499–507. http://dx.doi.org/10.1007/978-1-4615-4153-0_51.

Tinarelli, G., Anfossi, D., Brusasca, G., Ferrero, E., Giostra, U., Morselli, M., Moussafir, J., Tampieri, F., Trombetti, F., 1994. Lagrangian particle simulation of tracer dispersion in the lee of a schematic 2-dimensional hill. J. Appl. Meteorol. 33, 744–756. http://dx.doi.org/10.1175/1520-0450(1994)033<0744:LPSOTD>2.0.CO;2.

Tinarelli, G., Mortarini, L., Trini Castelli, S., Carlino, G., Moussafir, J., Olry, C., Armand, P., Anfossi, D., 2012. Review and validation of MicroSpray, a Lagrangian particle model of turbulent dispersion. In: Lin, J., Brunner, D., Gerbig, C., Stohl, A., Luhar, A., Webley, P. (Eds.), Lagrangian Modeling of the Atmosphere. p. 311+. http://dx.doi.org/10.1029/2012GM001242, AGU Chapman Conference on Advances in Lagrangian Modeling of the Atmosphere, Grindelwald, Switzerland, OCT (2011) 09-14.

Tinarelli, G., Uboldi, F., Carlino, G., 2018. Source term estimation using an adjoint model: a comparison of two different algorithms. Int. J. Environ. Pollut. 64, 209–229. http://dx.doi.org/10.1504/IJEP.2018.099157.

Trini Castelli, S., Armand, P., Tinarelli, G., Duchenne, C., Nibart, M., 2018. Validation of a Lagrangian particle dispersion model with wind tunnel and field experiments in urban environment. Atmos. Environ. 193, 273–289. http://dx.doi.org/10.1016/j.atmosenv.2018.08.045.

Trini Castelli, S., Bisignano, A., Donateo, A., Landi, T.C., Martano, P., Malguzzi, P., 2020. Evaluation of the turbulence parametrization in the MOLOCH meteorological model. Q. J. R. Meteorol. Soc. 146, 124–140. http://dx.doi.org/10.1002/qj.3661.

Trini Castelli, S., Tinarelli, G., Uboldi, F., Malguzzi, P., Bonasoni, P., 2022. Developments of SPRAY Lagrangian particle dispersion model for tracing the origin of odour nuisance. In: Mensink, C., Jorba Casellas, O. (Eds.), Air Pollution Modeling and Its Application XXVIII. Springer, Cham pp. 35–41. http://dx.doi.org/10.1007/978-3-031-12786-1_5.

Uboldi, F., Trini Castelli, S., Tinarelli, G., Malguzzi, P., Drofa, O., Bonasoni, P., 2022. H21-088: A novel approach for tracing the origin of odour nuisance with SMART meteo-dispersive modelling system. In: Proceedings of the 21st International Conference on Harmonisation Within Atmospheric Dispersion Modelling for Regulatory Purposes. HARMO 2022, pp. 632–637.